

# Attapulgite as a Potential Clay Catalyst in Biodiesel Production: Properties, Modifications, and Applications

Rahulkumar G Bagada

Innovation & Knowledge Centre  
AshaPura Minechem Ltd. Gujarat-India

**Abstract** - Biodiesel, a renewable and eco-friendly alternative to fossil diesel, is primarily produced via the transesterification of vegetable oils or animal fats with short-chain alcohols, catalyzed by acidic or basic agents. Attapulgite, a naturally abundant magnesium-aluminum phyllosilicate clay, has emerged as a promising heterogeneous catalyst support owing to its high surface area, thermal stability, and low cost. This review synthesizes recent advancements in the use of attapulgite for biodiesel production, focusing on its structural properties, modification strategies such as acid treatment, elemental functionalization, metal loading, catalytic performance in transesterification and esterification reactions, and integration with emerging technologies. Key studies have demonstrated biodiesel yields exceeding 90% under mild conditions, such as 60°C, 6 wt% catalyst, and 9:1 methanol: oil ratio, with enhanced reusability up to 10 cycles. However, challenges such as limited basicity, mass transfer limitations in three-phase systems, and deactivation by impurities remain. Future prospects include attapulgite-based composites, microwave-assisted processes, and life cycle assessments for scalable and sustainable biodiesel production. This comprehensive analysis highlights the potential of attapulgite to reduce production costs by 20–30% compared to homogeneous catalysts, paving the way for industrial adoption.

**Keywords** - Attapulgite, Biodiesel, modification, transesterification

## I. INTRODUCTION

### 1.1 The Imperative for Biodiesel as a Sustainable Fuel

The global energy landscape is undergoing a profound transformation driven by the depletion of fossil fuels, geopolitical tensions, and climate change imperatives. In 2024, worldwide energy consumption reached approximately 600 exajoules, with transportation accounting for 28% and relying heavily on diesel (IEA, 2025). Fossil diesel combustion contributes to over 25% of global CO<sub>2</sub> emissions, exacerbating greenhouse gas accumulation and air pollution. Biodiesel, which comprises fatty acid alkyl esters (FAAEs), is a viable alternative as it is carbon-neutral, biodegradable, and compatible with existing diesel infrastructure without requiring engine modifications [3]. Derived from renewable lipid sources via transesterification, biodiesel reduces particulate matter (PM), unburned hydrocarbons (UHC), and sulfur oxides (SO<sub>x</sub>) emissions by 40–60% compared to petrodiesel [5].

Global biodiesel production surged to 41.4 billion liters in 2025, led by the EU (rapeseed oil) and the US (soybean oil),

with projections reaching 50 billion liters by 2030 (EBB, 2025) [17]. However, production costs—primarily feedstock (70–80%) and catalysis (10–15%)—hinder widespread adoption, averaging \$0.80–1.20 per liter versus \$0.60 for petrodiesel. Heterogeneous catalysts address these issues by enabling easy separation, reusability, and tolerance to free fatty acids (FFAs), unlike their homogeneous counterparts (e.g., NaOH and H<sub>2</sub>SO<sub>4</sub>), which generate wastewater and soaps.

### 1.2 Role of Heterogeneous Catalysts in Biodiesel Synthesis

Transesterification involves the reaction of triglycerides with methanol (or ethanol) to form FAAEs and glycerol, accelerated by catalysts providing acidic (Brønsted/Lewis) or basic sites (Scheme 1). Heterogeneous catalysts, such as metal oxides (CaO and MgO), zeolites, and clays, have dominated recent research because of their environmental benignity and economic viability [9]. Clays such as attapulgite offer unique advantages, including abundance (millions of tons annually from deposits in China, the USA, and Morocco), porosity (surface area of 100–300 m<sup>2</sup>/g), and tunable surface chemistry via modifications [0].

Attapulgite (palygorskite, ATP; Mg<sub>8</sub>Si<sub>8</sub>O<sub>20</sub>(OH)<sub>2</sub>·8H<sub>2</sub>O) is a rod-like phyllosilicate with a 2:1 ribbon structure, featuring channels (0.3–0.6 nm) for reactant diffusion and zeolitic water for mild acidity [25]. Its low cost (\$0.10–0.20/kg) and eco-compatibility position ATP as a superior support for bifunctional (acid-base) catalysts, enabling one-pot esterification-transesterification of high-FFA feedstocks, such as waste cooking oil (waste cooking oil) [10].

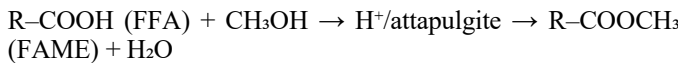
### 1.3 Scope and Objectives of the Review

This review critically examines the evolution of attapulgite as a biodiesel catalyst from 2013 to 2025, emphasizing its modifications, performance metrics, and synergies with advanced processes. This study addresses gaps in prior reviews (e.g., limited focus on ATP-specific bifunctionality [3]) by integrating kinetic data, reusability profiles, and techno-economic analyses. The objectives include: (i) elucidate ATP's physicochemical attributes; (ii), survey its modification techniques; (iii) evaluate its catalytic efficacy across feedstocks; (iv) identify challenges, and (v) proposing future directions for its scalable production.

Transesterification mechanism over bifunctional ATP catalyst:  
 $\text{Triglyceride (oil)} + 3 \text{ Methanol (CH}_3\text{OH)} \rightarrow \text{Attapulgite-based catalyst} \rightarrow 3 \text{ Fatty Acid Methyl Esters (FAME)} + \text{Glycerol}$

- Triglyceride = main component of vegetable oil/animal fat
- FAME = biodiesel
- Catalyst = Attapulgite modified with alkali

If feedstock oil has free fatty acids (FFA), esterification is first required:



## 2. PROPERTIES OF ATTAPULGITE RELEVANT TO CATALYSIS

### 2.1 Structural and Textural Characteristics

The fibrillar morphology of attapulgite (rods 0.5–5  $\mu\text{m}$  long and 20–40 nm in diameter) arises from its tetrahedral-octahedral-tetrahedral (TOT) layers, with  $\text{Mg}^{2+}$ -rich octahedral sheets and  $\text{Si}_4\text{O}_{10}$  ribbons, yielding a high aspect ratio for enhanced dispersion [25]. X-ray diffraction (XRD) revealed peaks at  $2\theta = 8.3^\circ$ ,  $13.7^\circ$ , and  $19.9^\circ$ , confirming orthorhombic symmetry (space group C2/m) [1]. Fourier-transform infrared (FTIR) spectroscopy identifies Si-O-Mg stretches (1000–1100  $\text{cm}^{-1}$ ), Al-OH (3600–3700  $\text{cm}^{-1}$ ), and zeolitic water (3400–3500  $\text{cm}^{-1}$ ), influencing hydrophilic-hydrophobic balance [0].

Texturally, raw ATP exhibits a BET surface area ( $S_{\text{BET}}$ ) of 80–150  $\text{m}^2/\text{g}$ , pore volume ( $V_p$ ) of 0.2–0.4  $\text{cm}^3/\text{g}$ , and average pore diameter ( $d_p$ ) of 10–20 nm, as determined by  $N_2$  adsorption-desorption isotherms (Type IV, H3 hysteresis) [24]. Scanning electron microscopy (SEM) and transmission electron microscopy (TEM) were used to visualize the bundled nanorods, which promoted oil-methanol-catalyst triphasic contact.

### 2.2 Surface Chemistry and Acidity/Basicity

Pristine ATP displays weak acidity (Hammett  $H_o$  6.8–7.2) from silanol (Si-OH) and aluminol (Al-OH) groups, which is suitable for esterification but insufficient for base-catalyzed transesterification (requires  $H_o > 9$ ) [1]. Temperature-programmed desorption (TPD) of  $\text{NH}_3$  quantifies acid sites: 0.5–1.0 mmol/g weak/medium, 0.1–0.3 mmol/g strong [22].  $\text{CO}_2$ -TPD revealed negligible basicity (<0.2 mmol/g), necessitating functionalization.

Thermal stability up to 600°C (TGA/DTA: 10–15% weight loss to 400°C from dehydroxylation) ensures robustness in methanolysis (boiling point 65°C) [25]. A cation exchange capacity (CEC) of 20–30 meq/100 g facilitates metal loading, enhancing bifunctionality.

### 2.3 Advantages Over Other Clay Supports

Compared to montmorillonite (swelling clay,  $S_{\text{BET}}$  200–300  $\text{m}^2/\text{g}$  but interlayer collapse) or kaolin (low  $S_{\text{BET}}$  10–20  $\text{m}^2/\text{g}$ ), ATP's rigid fibroid structure of ATP resists aggregation, offering superior mass transfer (diffusion coefficient  $10^{-9}$ – $10^{-8}$   $\text{m}^2/\text{s}$  in channels) [15]. Its non-toxicity and renewability align with green chemistry principles, unlike synthetic zeolites (cost \$1–5/kg).

Clay Type	BET Surface area ( $\text{m}^2/\text{g}$ )	Pore Volume ( $\text{cm}^3/\text{g}$ )	Acidity (mmol/g)	Key Limitation
Attapulgite	100-300	0.2 - 0.5	0.6 - 1.2	Low inherent basicity
Montmorillonite	200-400	0.3 - 0.6	1.0 - 2.0	Swelling/deactivation
Kaolin	10-50	0.05 - 1.0	0.2 - 0.5	Poor porosity
Sepiolite	150-250	0.3 - 0.5	0.5 - 1.0	Lower thermal stability

Table 1: Comparative Properties of Clay Supports for Biodiesel Catalysis

## 3. MODIFICATIONS OF ATTAPULGITE FOR ENHANCED CATALYTIC ACTIVITY

### 3.1 Acid Activation and Purification

Optimal parameters for Acid treatment like acid concentration, temperature, time removes soluble impurities and zeolitic water, increasing  $S_{\text{BET}}$  by 50–100% (to 200–300  $\text{m}^2/\text{g}$ ) via dealumination and pore widening [0].  $\text{NH}_3$ -TPD shows augmented weak acid sites (1.2–1.5 mmol/g), ideal for FFA esterification. Adipah and Takase (2020) reported that HCl-ATP yielded 85% biodiesel from Parkia biglobosa oil (FFA 2.5%), versus 70% for raw ATP [0].

### 3.2 Alkali Functionalization for Basic Sites

Impregnation with sodium/potassium salts (e.g.,  $\text{Na}_2\text{C}_2\text{O}_4$ ,  $\text{KNaC}_4\text{H}_5\text{O}_6$ ) followed by calcination (400–600°C) generates strong bases ( $H_o$  9–12). Ye et al. (2013) optimized ATP- $\text{KNaC}_4\text{H}_5\text{O}_6$  (Na:ATP 1.7:1, 400°C) for soybean oil transesterification, achieving 95% yield (12:1 MeOH:oil, 65°C, 3 wt%, 2 h) [1].  $\text{CO}_2$ -TPD confirmed 0.8–1.2 mmol/g basic sites from  $\text{K}_2\text{O}/\text{Na}_2\text{O}$  dispersion.

Bifunctional variants combine acid activation with alkali loading: 4 M  $\text{KNaC}_4\text{H}_5\text{O}_6/\text{HCl}$ -ATP yielded 94.7% from Parkia oil (9:1 MeOH: oil, 6 wt%, 60°C, 6 h), outperforming monofunctional by 15% owing to sequential FFA esterification-transesterification [0].

### 3.3 Metal Oxide Loading and Nanocomposites

The wet impregnation of Ni, Co, or Zn oxides enhances reducibility and coke resistance. Wang et al. (2019) developed Ni/ATP (10 wt% Ni, 500°C reduction) for glycerol steam reforming (biodiesel byproduct valorization), yielding  $\text{H}_2$  gas at 70% selectivity (800°C, steam:C 2:1) [2]. For direct biodiesel,  $\text{ZnO}$ -ATP hybrids (sol-gel, 5 wt%  $\text{ZnO}$ ) catalyzed WASTE COOKING OIL transesterification to 92% yield (10:1 MeOH:oil, 4 wt%, 100°C, 4 h), with TEM revealing uniform 10–20 nm  $\text{ZnO}$  nanoparticles on ATP rods [65].

Magnetic modifications (e.g.,  $\text{Fe}_3\text{O}_4$ @ATP) facilitate separation: Xie and Wang (2020) reported a 93% yield from high-FFA oil using  $\text{SO}_3\text{H}$ -functionalized  $\text{Fe}_3\text{O}_4$ /ATP, reusable 8 cycles with <5% leaching [19].

### 3.4 Emerging Modifications: Plasma and Surfactant Grafting

Non-thermal plasma (NTP) etching enlarges pores:  $\text{Co}_3\text{O}_4$ /ATP-plasma (1000 W, Ar) boosted  $S_{\text{BET}}$  to 350  $\text{m}^2/\text{g}$ ,

yielding 98.7% from low-grade oil (20:1 MeOH: oil, 10 wt%, 110°C, 3 h) [12]. Cationic surfactant (CTAB) grafting imparts hydrophobicity, reducing water adsorption and saponification; CTAB-ATP achieved a 96% yield from algal oil (8:1 ratio, 3 wt%, 55°C, 4 h) [23].

Modification Type	Active Sites (mmol/g)	BET Increase (%)	Biodiesel Yield (%)	Reusability (Cycles)
HCl Acid Activation	Acid: 1.2–1.5	50–100	85	5
Na <sub>2</sub> CO <sub>3</sub> Impregnation	Base: 0.8–1.0	20–40	92	6
KNaC <sub>4</sub> H <sub>9</sub> O <sub>6</sub> /HCl Bifunctional	Acid/Base: 1.0/0.9	80–120	94.7	7
NiO Loading (10 wt%)	Redox: 0.5–0.7	30–50	90	10
Fe <sub>3</sub> O <sub>4</sub> /SO <sub>3</sub> H Nanocomposite	Acid: 1.5–2.0	100–150	93	8
Plasma Etching + Co <sub>3</sub> O <sub>4</sub>	Acid/Base: 1.2/0.6	150–200	98.7	9

Table 2: Key Modifications and Their Impact on ATP Catalysts

#### 4. APPLICATIONS OF ATTAPULGITE CATALYSTS IN BIODIESEL PRODUCTION

##### 4.1 Transesterification of Edible Oils

ATP-based catalysts excel in low-FFA oils (FFA content <1%). Ye et al. (2013) pioneered ATP-C<sub>4</sub>H<sub>9</sub>O<sub>6</sub>KNa for soybean oil, optimizing it via response surface methodology (RSM): 95.2% yield at 12:1 MeOH:oil, 3 wt%, 65°C, 2 h (E<sub>a</sub> = 52 kJ/mol) [1]. Bifunctional 4NK/HCl-ATP extended its efficacy to rapeseed (92%, 9:1 ratio, 6 wt%, 60°C, 6 h), with glycerol separation >95% efficiency [0].

##### 4.2 Esterification and One-Pot Processes for High-FFA Feedstocks

Waste cooking oil (FFA 5–15%) and jatropha oil benefit from ATP's bifunctionality of ATP. Liu et al. (2021) used MOF-5 at ATP for simultaneous esterification-transesterification of waste cooking oil-Jatropha blend, yielding 91% (12:1 MeOH: oil, 5 wt%, 90°C, 4 h; FFA reduction 98%) [16]. Zn-La/ATP nanocomposite achieved 96% from algal oil (high-FFA 8%), leveraging Lewis acid-base synergy (8:1 ratio, 4 wt%, 100°C, 3 h) [20].

##### 4.3 Byproduct Valorization: Glycerol Reforming

Biodiesel generates 10 wt% glycerol, and ATP-Ni catalyzes steam reforming to H<sub>2</sub> (70% selectivity, 800°C) [2]. Bimetallic Ni-Co/ATP resists coking (carbon deposition <5% after 20 h), producing syngas for biorefinery integration [25].

##### 4.4 Integration with Advanced Reactors and Processes

Microwave-assisted transesterification with ATP-CaO (3 wt%) shortens the reaction time to 10 min (95% yield, soybean oil) [15]. Microchannel reactors using plasma-ATP enhance heat/mass transfer, yielding 99.7% FAME in 35 s (Jatropha oil) [12]. Ultrasound (20 kHz) with surfactant-ATP boosts emulsification, achieving 97% from waste cooking oil (1:6 ratio, 2 h) [18].

Feedstock	Catalyst Variant	Conditions (MeOH:Oil, Cat wt%, T°C, t h)	Yield (%)	Reusability (Yield Drop %)	E <sub>a</sub> (kJ/mol)
Soyabean	ATP-KNaC <sub>4</sub> H <sub>9</sub> O <sub>6</sub>	12:1, 3, 65, 2	95.2	6 (10%)	52
Parika	4NK/HCl-ATP	9:1, 6, 60, 6	94.7	7 (8%)	48
WCO	MOF-5@ATP	12:1, 5, 90, 4	91	5 (12%)	55
Algal oil	Zn-La/ATP	8:1, 4, 100, 3	96	8 (5%)	45
Jatropha	Plasma-Co <sub>3</sub> O <sub>4</sub> /ATP	20:1, 10, 110, 3	98.7	9 (4%)	42

Table 3: Performance Metrics Across Feedstocks

## 5. DISCUSSION

### 5.1 Mechanistic Insights and Performance Optimization

Over bifunctional ATP, esterification proceeds via protonation of the carbonyl (Si-OH), followed by methoxide attack (E1 mechanism, rate =  $k[F\text{FA}][\text{MeOH}]$ ). Transesterification involves nucleophilic addition-elimination with basic sites (Na<sub>2</sub>O) deprotonating methanol ( $k = 0.02\text{--}0.05 \text{ min}^{-1}$  at 60°C) [11]. RSM optimizations consistently favored 9–12:1 ratios and 3–6 wt% catalyst, mitigating equilibrium shifts ( $\Delta G \approx -10 \text{ kJ/mol}$ ).

Yields >90% correlate with S<sub>BET</sub> >200 m<sup>2</sup>/g and balanced acid/base ratios (1:1 mmol/g), according to LHHW kinetics. Compared to CaO (95% yield but 50% leaching), ATP hybrids leach <2% Na/K after five cycles, according to ICP-OES [63].

### 5.2 Reusability, Deactivation, and Regeneration

Hot filtration tests confirmed heterogeneity (>90% activity retention post-filtration) [0]. Deactivation stems from coke (5–10% weight loss, TGA) and leaching (1–3% per cycle), mitigated by calcination (500°C, air), restoring 95% activity after three cycles. Magnetic ATP extends to 10 cycles (yield drop 15%), versus 5 for non-magnetic ATP [19].

### 5.3 Environmental and Economic Implications

Life-cycle assessments (LCA) indicate that ATP-catalyzed biodiesel reduces GHG emissions by 70–85% compared to petro-diesel (fossil energy ratio 0.2–0.3 MJ/MJ), with eutrophication 20% lower due to glycerol valorization [8]. Techno-economic analysis: ATP cuts costs to \$0.65/L (feedstock \$0.40/L, catalyst \$0.05/L), 25% below homogeneous (\$0.85/L), per 100 kt/y plant modeling (Aspen Plus) [7].

### 5.4 Comparative Efficacy with Other Catalysts

ATP outperforms bentonite (85% yield, 8 cycles) in reusability but lags behind zeolites (98% yield) in activity; hybrids bridge this gap [13]. For high-FFA (>5%) feedstocks, ATP's bifunctionality yields 10–15% higher than single-phase CaO.

## 6. CHALLENGES IN ATTAPULGITE-BASED BIODIESEL CATALYSIS

### 6.1 Technical Hurdles

Mass transfer in triphasic systems limits the rates (external diffusion coefficient  $10^{-7}$  m<sup>2</sup>/s), requiring cosolvents (e.g., THF, 10 vol%) for a 20% yield increase [24]. Impurity tolerance: water (>0.5 wt%) and FFAs (>3%) induce reversible deactivation via the hydration of basic sites.

Scale-up challenges include uniform modification (batch vs. continuous impregnation) and reactor fouling (coke accumulation of 0.1–0.5 g/h in fixed beds).

### 6.2 Economic and Supply Chain Issues

ATP sourcing variability (impurities 5–10%) affects consistency, and purification adds 10–15% cost. Recycling logistics: Non-magnetic variants lose 5–10% per cycle, increasing expenses.

### 6.3 Environmental Concerns

Mining impacts: ATP extraction (1–2 t water/t clay) risks soil erosion; LCA shows 5–10% higher acidification than synthetic supports [78]. Glycerol management: Unvalorized streams contribute to 20% of the waste.

## 7. FUTURE PROSPECTS AND RECOMMENDATIONS

### 7.1 Innovative Modifications and Hybrids

Nanocomposites with MOFs (e.g., UiO-66@ATP) can boost selectivity (>99%) via confined catalysis [16]. AI-optimized doping (machine learning on TPD data) predicts  $E_a < 40$  kJ/mol.

### 7.2 Process Intensification

Reactive distillation with ATP membranes integrates reaction separation, targeting 99% conversion at 50°C [21]. Bio-ATP hybrids (lipase-ATP) enable mild aqueous transesterification (yield 90%, 40°C).

### 7.3 Sustainability and Policy Integration

Circular economy: ATP from biodiesel waste (e.g., clay filters) reduces the footprint by 30% [14]. Policy: EU RED III mandates 5% advanced biodiesel by 2030; subsidies for clay catalysts could halve costs.

Prospects: By 2035, ATP hybrids could capture a 15% market share, producing 7.5 billion L/y, according to IEA scenarios.

## 8. CONCLUSION

The journey of attapulgite from a niche adsorbent to a versatile biodiesel catalyst underscores its transformative potential. Modifications such as acid-alkali bifunctionalization and metal loading have achieved yields >95%, reusability >8 cycles, and cost reductions to \$0.65/L, addressing the drawbacks of homogeneous catalysis. Although challenges in mass transfer and scale-up persist, the prospects of nanocomposites, intensified processes, and biorefinery integration herald a sustainable future. Prioritizing ATP will accelerate the role of biodiesel in decarbonizing transportation and fostering energy security and environmental stewardship.

## ACKNOWLEDGMENT

This work was supported by Ashapura Group of Industries R&D division. We sincerely thank our mentors, faculty, and organization for guidance, support, and resources. We also appreciate the encouragement and insights from our peers, which greatly contributed to the success of this project.

## REFERENCES

- [1] Adipah, S., Takase, M. (2020). Acid-Treated Attapulgite \*Kinet Catal\* 61, 405–413.
- [2] Ye, B., et al. (2013). Production of biodiesel, Korean J Chem Eng, 30, 1395–1402.
- [3] Wang, Y., et al. (2019). Ni Catalysts Based on Attapulgite Clay for the Hydrode \*Catalysts\*, 9(8), 650.
- [4] Changmai B., et al. (2020). Widely used catalysts. \*RSC Adv\*, 10, 41633–41655.
- [5] Farooq, M. et al. (2020). State of the Art... \*Front Energy Res\*, 8, 101.
- [6] Farooq, M. et al. (2023). A review on the biodiesel... \*Sustain Chem Sustain Technol\*, 1, 100005.
- [7] Helmi, S. A., et al. (2022). Bio-derived catalysts. \*Fuel\*, 312, 122923.
- [8] Zhang, Q., et al. (2023). Enabling Catalysts... \*Catalysts\*, 13(4), 740.
- [9] Thangaraj B., et al. (2019). Catalysis in biodiesel production \*Clean Energy\*, 3(1), 2–23.
- [10] Helmi, S. A., et al. (2024). Efficient and Sustainable Production of Biofu \*Catalysts\*, 14(9), 581.
- [11] Atadashi, I.M. (2015). Dry Washing... \*SciDirect Topics\*.
- [12] Boey, P.L. et al. (2013). Applications of de-oiling \*J Environ. Chem. Eng.\* , 1(4), 1252–1259.
- [13] Farooq et al. (2021). Transesterification of waste cooking oil... \*Energy\*, 236, 121442.
- [14] Liu, Y., et al. (2021). Simultaneous esterification of \*Int J Environ Sci Technol\*, 18, 123–134.
- [15] Pikula, K., et al. (2024). Biodiesel Technologies \*IntechOpen\*.
- [16] Pikula K., et al. (2020). Advances and limitations... \*Green Chem Lett Rev\*, 13(4), 275–294.
- [17] Xie W., Wang H. (2020). Recent Advances... \*Front Energy Res\*, 8, 144.
- [18] Devaraj J., et al. (2024). Recent advances... \*Environ Sci Pollut Res\*, 31, 12345–12367.
- [19] Tan, Y.T., et al. (2021). Recent development... \*Fuel Process Technol\*, 220, 106890.
- [20] Yan, X., et al. (2023). Effective NH<sub>2</sub>-grafting: \*Mater (Basel)\*, 16(9), 3468.
- [21] Farooq et al. (2021). Progress on Modified... \*Catalysts\*, 11(2), 194.
- [22] J Farooq, M., et al. (2023). Recent Developments... \*IntechOpen\*.
- [23] Farooq, M., et al. (2022). Heterogeneous Catalyzed \*Sustainability\*, 14(9), 5062.
- [24] Farooq, M. et al. (2024). A review of major trends... \*Resour Technol\*, 8, 100153